Combined effect of heat generation or absorption and first-order chemical reaction on micropolar fluid flows over a uniformly stretched permeable surface

Rebhi A. Damseh [a,*], M.Q. Al-Odat [a], Ali J. Chamkha [b], Benbella A. Shannak [a]

[a] *Mechanical Engineering Department, Al-Huson University College, Al-Balqa Applied University, P.O. Box 50, Irbid, Jordan*
[b] *Manufacturing Engineering Department, The Public Authority for Applied Education and Training, P.O. Box 42325, Shuweikh 70654, Kuwait*

A R T I C L E   I N F O

A B S T R A C T

This work is focused on the study of combined heat and mass transfer by natural convection of a micropolar, viscous and heat generating or absorbing fluid flow near a continuously moving vertical permeable infinitely long surface in the presence of a first-order chemical reaction. The governing equations for this investigation are formulated and solved numerically using the fourth-order Runge–Kutta method. Comparisons with previously published work on special cases of the problem are performed and found to be in excellent agreement. A parametric study illustrating the influence of the micro-gyration parameter, vortex viscosity parameter, chemical reaction parameter, Schmidt number, heat generation or absorption parameter on the fluid velocity as well as the skin-friction coefficient and the Nusselt and Sherwood numbers is conducted. The results of this parametric study are shown graphically and the physical aspects of the problem are highlighted and discussed.

1. Introduction

In recent years, the dynamics of micropolar fluids has been a popular area of research. As the fluids consist of randomly oriented molecules, and as each volume element of the fluid has translation as well as rotation motions, the analysis of physical problems in these fluids has revealed several interesting phenomena, which are not found in Newtonian fluids. The theory of micropolar fluids and thermo micropolar fluids developed by Eringen [1,2] can be used to explain the characteristics in certain fluids such as exotic lubricants, colloidal suspensions, or polymeric fluids, liquid crystals and animal blood. The micropolar fluids exhibit certain microscopic effects arising from local structure and microrotation of fluid elements. An excellent review about micropolar fluid mechanics was provided by Ariman et al. [3,4].

In the past decades, the researchers have focused mainly on the heat transfer of micropolar fluid flow over flat plates [5–7] or regular surfaces [8,9]. Recently, Nazar et al. [10] studied mixed convection heat transfer from a horizontal circular surface. Cheng and Wang [11] studied the effect of wavy surfaces on micropolar fluids forced convection heat transfer. They found that increasing the micropolar fluid parameter resulted in decreasing the heat transfer rates and increasing the local coefficient of friction and the hydrodynamic and thermal boundary layer thicknesses. Bhargava and

Takhar [12] studied micropolar boundary layer near a stagnation point on a moving wall. They found that the temperature increased inside the boundary layer compared to the Newtonian fluid flow case. Mansour et al. [13] studied heat and mass transfer effects on magnetohydrodynamic flow of micropolar fluid on a circular cylinder with uniform heat and mass flux. Their results indicated that the micropolar fluids displayed a reduction in drag as well as heat transfer when compared with those of Newtonian fluids. Kelson and Desseaux [14] reported self-similar solutions for the boundary layer flow of micropolar fluids driven by a stretching sheet with uniform suction or blowing through the surface. Ibrahim and Hassanien [15] obtained local similarity solutions for mixed convection boundary layer flow of a micropolar fluid on horizontal flat plates with variable surface temperature. Kim and Lee [16] developed analytical studies on MHD oscillatory flow of a micropolar fluid over a vertical porous plate. The effects of non-zero values of micro-gyration vector on the velocity and temperature fields across the boundary layer were studied using the method of small perturbation approximation.

The study of heat and mass transfer in moving fluid is important in view of several physical problems, such as fluids undergoing exothermic and endothermic chemical reaction. In many chemical engineering processes, chemical reactions take place between a foreign mass and the working fluid which moves due to the stretching of a surface. The order of the chemical reaction depends on several factors. One of the simplest chemical reactions is the first-order reaction in which the rate of reaction is directly proportional to the species concentration. Chamkha [17] studied the problem of heat and mass transfer by steady flow of electri-

---

* Corresponding author.

E-mail addresses: rdamseh@yahoo.com (R.A. Damseh), achamkha@yahoo.com (A.J. Chamkha).

Nomenclature

B	dimensionless material parameter
C	concentration
c_p	specific heat of the fluid at constant pressure
C_f	coefficient of friction
D	mass diffusion coefficient
g	magnitude of acceleration due to gravity
Gr_C	mass Grashof number, $Gr_C = gB_C\upsilon(C_W - C_\infty)/u_w v_w^2$
Gr_T	thermal Grashof number, $Gr_T = gB_T\upsilon(T_W - T_\infty)/u_w v_w^2$
j	micro-inertia density
k	thermal conductivity
M	dimensionless material parameter
m	dimensionless micro-gyration vector
N	dimensionless micro-rotation variable
Nu	Nusselt number
Pr	Prandtl number, υ/α
Q	dimensionless heat generation or absorption parameter
q_c	dimensional heat generation or absorption coefficient
R	vortex viscosity parameter
T	temperature
Sc	Schmidt number
Sh	Sherwood number
u	fluid axial velocity

U	dimensionless velocity
v	transverse velocity
x, y	axial and transverse coordinates
X, Y	dimensionless coordinates

Greek symbols

α	chemical reaction parameter
β_C	coefficient of concentration expansion
β_T	coefficient of thermal expansion
Λ	spin gradient viscosity
κ	vortex viscosity
λ	dimensionless material parameter
θ	non-dimensional temperature
φ	non-dimensional concentration
γ	dimensionless chemical reaction parameter.
μ	dynamic viscosity
υ	kinematic viscosity
ρ	fluid density
ω	micro-rotation component

Subscripts

∞	free stream condition
w	condition at the wall

---

cally conducting fluid on a uniformly moving vertical surface in the presence of first-order chemical reaction. Kandasamy et al. [18] studied the nonlinear MHD flow with heat and mass transfer characteristics of an incompressible, viscous, electrically conducting fluid on a vertical stretching surface with chemical reaction and thermal stratification effects. They also reported a numerical solution for the steady laminar boundary-layer flow over a wall of the wedge with suction or injection in the presence of species concentration and mass diffusion [19]. Other examples of studies dealing with chemical reactions can be found in the papers by Pradeep et al. [20], Mitrovic et al. [21] and Chen et al. [22].

The aim of the present work is to investigate natural convection heat and mass transfer adjacent to a continuously moving vertical porous infinite plate for incompressible, micropolar fluid in the presence of heat generation or absorption effects and a first-order chemical reaction.

2. Mathematical formulation

Consider steady, laminar, heat and mass transfer by natural convection boundary layer flow of a micropolar fluid above a continuously moving vertical infinite porous plate in the presence of heat generation or absorption and a first-order chemical reaction. The particle size of the micropolar fluid is sufficiently small compared with the hole size of porous plate. The problem is described in a rectangular coordinate system attached to the plate such that the x-axis lies along the plate surface and the y-axis is normal to the plate. The plate is assumed to be infinitely long so that all dependent variables are only functions of y. The micropolar fluid is assumed to be viscous and has constant properties except the density in the buoyancy term of the balance of linear momentum equation. The temperature and the concentration at the plate surface are always greater than their free stream values.

The governing boundary-layer equations are based on the continuity, linear momentum, micro-rotation, energy and solute concentration equations taking into account the presence of heat generation or absorption and a chemical reaction in addition to

the Boussinesq approximation. Considering the above assumptions, these equations can be written as follows:

$$\frac{\partial v}{\partial y} = 0 \tag{1}$$

$$\left(v \frac{\partial u}{\partial y}\right) = (\upsilon + \kappa)\frac{\partial^2 u}{\partial y^2} + \kappa \frac{\partial \omega}{\partial y} + g\beta_T(T - T_\infty) + g\beta_C(C - C_\infty) \tag{2}$$

$$\rho j\left(v \frac{\partial \omega}{\partial y}\right) = \kappa\left(-\frac{\partial u}{\partial y} - 2\omega\right) + \Lambda\frac{\partial^2 \omega}{\partial y^2} \tag{3}$$

$$\rho c_p\left(v \frac{\partial T}{\partial y}\right) = k\frac{\partial^2 T}{\partial y^2} - q_c(T - T_\infty) \tag{4}$$

$$v \frac{\partial C}{\partial y} = D\frac{\partial^2 C}{\partial y^2} - \alpha(C - C_\infty) \tag{5}$$

It should be mentioned that the last two terms in Eq. (2) represent thermal and solutal buoyancy effects, respectively. Also, the last term in Eq. (4) represents the heat generation or absorption effect while the last term in Eq. (5) represents a first-order chemical reaction.

The physical boundary conditions for the problem are:

$$\begin{cases} u = u_w, \ v = -v_w, \ \omega = -n(\partial u/\partial y), \ T = T_w, \ C = C_w \\ \quad \text{for } y = 0 \\ u = 0, \ \omega = 0, \ T = T_\infty, \ C = C_\infty \\ \quad \text{for } y \to \infty \end{cases} \tag{6}$$

In Eq. (6), the boundary condition for the micro-rotation variable ω at the wall is proportional to the surface shear stress, the proportional parameter n ranges between 0 and 1. The value for $n = 0$ corresponds to the case where the particle density is sufficiently large so that microelements close to the wall are unable to rotate. The value of $n = 0.5$ represents a weak representation of the microelements and the value of $n = 1.0$ corresponds to the turbulent flow inside boundary layers of micro-rotation.

Table 1
Effects of various parameters on C_f, Nu, and Sh numbers result in parenthesis [ ] is that of the analytical solution obtained by Chamkha [17].

Gr_T	Gr_C	Pr	Sc	Q	γ	C_f	Nu	Sh
1	1	0.71	0.6	0	0	2.0698 [2.0751]	0.7120 [0.7100]	0.6008 [0.6000]
1	1	0.71	0.6	0	2	1.0982 [1.1049]	0.7120 [0.7100]	1.4056 [1.4358]
1	1	0.71	2.0	1	2	0.4277 [0.4843]	1.2494 [1.2693]	1.4056 [1.4358]
1	1	0.71	0.6	−0.1	2	1.4102 [1.3926]	0.5911 [0.5896]	1.4056 [1.4358]
1	1	7.0	0.6	0	0	0.8502 [0.8095]	7.0160 [7.0000]	0.6008 [0.6000]
1	1	0.71	2.0	0	2	0.7094 [0.7175]	0.7120 [0.7100]	3.2194 [3.2361]

Defining the non-dimensional variables as

$$Y = (yv_w/\upsilon)$$

$$U = (u/u_w)$$

$$N = (\upsilon\omega/v_w u_w)$$

$$\theta = (T - T_\infty)/(T_w - T_\infty)$$

$$\varphi = (C - C_\infty)/(C_w - C_\infty) \tag{7}$$

and then substituting Eqs. (7) into Eqs. (1)–(5) yields the following dimensionless equations:

$$\frac{dU}{dY} + (1+R)\frac{d^2U}{dY^2} + R\frac{dN}{dY} + Gr_T\theta + Gr_C\varphi = 0 \tag{8}$$

$$\lambda\frac{d^2N}{dY^2} + \frac{dN}{dy} + RM\left(-\frac{dU}{dY} - 2N\right) = 0 \tag{9}$$

$$\frac{1}{Pr}\frac{d^2\theta}{dY^2} + \frac{d\theta}{dY} - Q\theta = 0 \tag{10}$$

$$\frac{1}{Sc}\frac{d^2\varphi}{dY^2} + \frac{d\varphi}{dY} - \gamma\varphi = 0 \tag{11}$$

where $R = \kappa/\mu$ is the vortex viscosity parameter, $M = \upsilon^2/jv_w^2$ and $\lambda = \Lambda/\mu j$ are dimensionless material parameters, $Pr = \mu c_p/k$, $Sc = \upsilon/D$, $Gr_T = gB_T\upsilon(T_w - T_\infty)/u_w v_w^2$, $Gr_C = gB_C\upsilon(C_w - C_\infty)/u_w v_w^2$ are the Prandtl number, Schmidt number, thermal Grashof number and mass Grashof number, respectively. $Q = \upsilon q_c/\rho c_p v_w^2$ is the dimensionless heat generation or absorption parameter and $\gamma = \alpha\upsilon/v_w^2$ is the dimensionless chemical reaction parameter.

The corresponding non-dimensional boundary conditions become

$$\begin{cases} U = 1, \ N = m(\partial U/\partial Y), \ \theta = \varphi = 1 & \text{for } y = 0 \\ U = 0, \ N = 0, \ \theta = \varphi = 0 & \text{for } y \to \infty \end{cases} \tag{12}$$

where $m = nu_w v_w/\upsilon$ is the dimensionless micro-gyration vector.

The skin-friction coefficient C_f, Nusselt and Sherwood numbers (Nu and Sh) are important physical parameters for this kind of flow. They are defined in dimensionless form by:

$$C_f = (1+R)\frac{dU}{dY}(0) + RN(0) \tag{13}$$

$$Nu = \frac{q_w\upsilon}{(T_w - T_\infty)kv_w} = -\frac{d\theta}{dY}(0); \quad q_w = -k\frac{dT}{dy}\bigg|_{y=0}$$

$$Sh = \frac{J_w\upsilon}{(C_w - C_\infty)Dv_w} = -\frac{d\varphi}{dY}(0); \quad J_w = -D\frac{dc}{dy}\bigg|_{y=0} \tag{14}$$

3. Results and discussion

The resulting ordinary differential equations (8)–(12) have been solved numerically by means of the fourth-order Runge–Kutta method with symmetric estimation of $U'(0)$, $N'(0)$, $\theta'(0)$ and $\varphi'(0)$ by the shooting technique. The basic step size used for the calculation is $\Delta Y = 5 \times 10^{-3}$. This value was arrived at after performing many numerical experiments to access grid independence. An iteration process is employed and continued until the desired results are obtained within the following convergence criterion

$$\left|\frac{f_{i+1} - f_i}{f_{i+1}}\right| \leqslant 10^{-6} \tag{15}$$

where f stands for U, ϕ, or θ and i refers to space coordinate.

In order to asses the accuracy of our method, we have compared our coefficient of friction C_f, Nusselt number Nu and Sherwood number Sh for $R = 0$ with the analytical solutions reported by Chamkha [17]. The analytical solution for Chamkha problem is given below

$$\theta = \exp(-m_1 y), \qquad \varphi = \exp(-m_2 y)$$

$$Nu = m_1, \qquad Sh = m_2 \tag{16}$$

where

$$m_1 = \frac{1}{2}\left[Pr + (Pr^2 + 4Pr\,Q)^{0.5}\right]$$

$$m_2 = \frac{1}{2}\left[Sc + (Sc^2 + 4Sc\,\gamma)^{0.5}\right] \tag{17}$$

The results are found to be in a good agreement and the comparison is presented in Table 1. It should be noted here that the vortex viscosity parameter R presented here is assigned a value of zero in order to have similar formulation between the current problem and that studied by Chamkha [17]. In addition, Figs. 4 and 6 present a good agreement between the analytically determined C_f and Nu values with those calculated from the present numerical code. These favorable comparisons lend confidence in the accuracy of the numerical results reported below.

Fig. 1 depicts the effect of the vortex viscosity parameter R ($R = 0, 1, 2, 3, 5$) on the dimensionless velocity profiles $U(Y)$ for the fixed values of $M = 0.5$, $Pr = 0.71$, $\lambda = 1.0$, $m = 0.0$, $Gr_T = 3.0$, $Gr_C = 1.0$, $Sc = 2.0$, $Q = -0.4$, $\lambda = 1.0$ and $\gamma = 0.6$. When $R = 0$, the linear momentum equation (8) is uncoupled from the angular momentum equation (9). For this case, the fluid velocity profile exhibits a distinctive peak close to the wall. However, for finite values of R, these equations are coupled. As the value of the vortex viscosity parameter increases, the coupling between Eqs. (8) and (9) increases causing a net reduction in the fluid velocity. This is due to extra mixing of fluid layers due to the enhanced shear stress. The peak value exhibited in the velocity profile decreases significantly close to the wall while the velocity away from the wall increases. This yields an increase in the boundary-layer thickness. These behaviors are clearly shown in Fig. 1.

The effect of the micro-gyration vector m on the velocity profiles is presented in Fig. 2. As the micro-gyration dimensionless parameter m increases, the angular rotation and the fluid velocity increase inside the boundary layer. The increase in the fluid velocity as m increases occurs with insignificant change in the boundary-layer thickness as seen from Fig. 2.

Table 2 illustrates the effects of R and m on the distributions of the skin-friction coefficient C_f. Inspection of Figs. 1 and 2 shows that the wall slope of the velocity profile decreases as R increases while it increases as m increases. However, this information is not
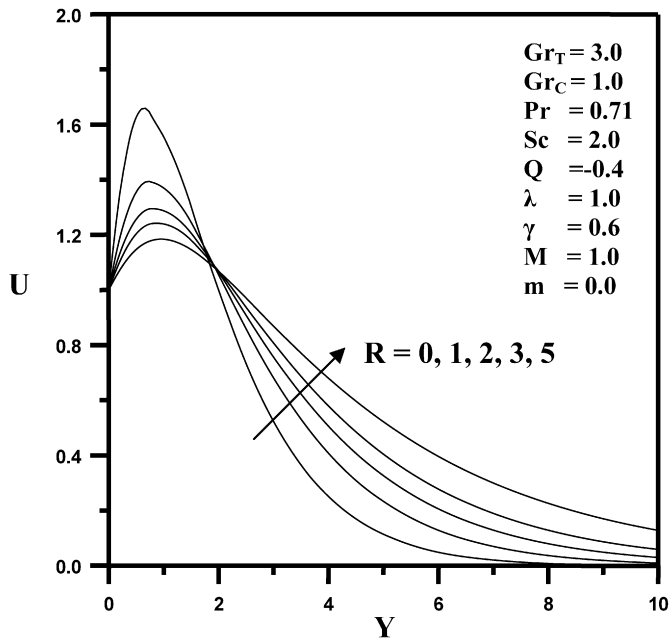
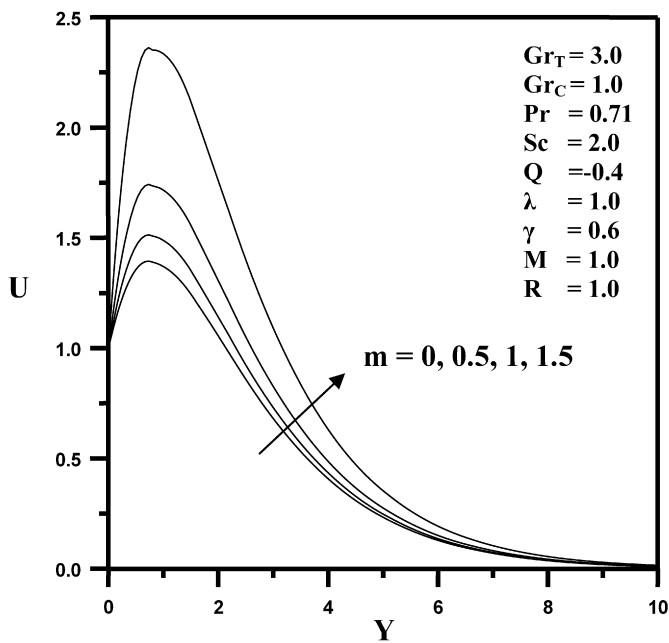**Fig. 1.** Effect of vortex viscosity parameter (R) on velocity distribution.

Fig. 2. Effect of dimensionless micro-gyration vector (m) on velocity distribution.

Table 2
Effects of micro-gyration vector and vortex viscosity parameter on coefficient of friction.

m	C_f $R=1$	C_f $R=2$	C_f $R=4$
0	2.3875	2.4062	2.4262
0.2	2.3828	2.3994	2.4092
0.4	2.3767	2.3908	2.3998
0.6	2.3717	2.3815	2.3852
0.8	2.3623	2.3634	2.3693
1.0	2.3490	2.3299	2.3310
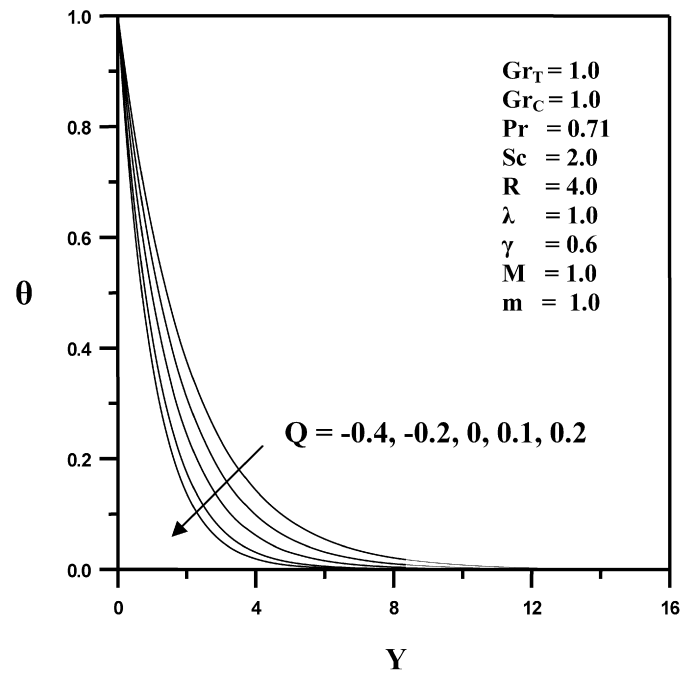
Fig. 3. Effect of heat generation or absorption parameter (Q) on temperature distribution.

enough to predict the behavior of C_f as either R or m increases. This is evident from the definition of C_f given in Eq. (13) as it is also dependent on the wall microrotation. For this situation, it is predicted that as R increases, the values of C_f increase due to extra fluid mixing while they decrease as m increases due to excessive angular momentum within fluid layers.

Fig. 3 presents typical temperature profiles for various values of the dimensionless heat generation or absorption parameter Q. The presence of heat generation within the boundary layer causes the energy level to increase. As a result, the temperature of the fluid increases everywhere away from the boundaries for which it is maintained constant there. In addition, the thermal boundary layer thickness and the negative wall slope of the temperature profile increase. On the other hand, the presence of heat absorption within the boundary layer produces the opposite effect, namely, decreases in the fluid temperature, the thermal boundary layer thickness and the negative wall slope of the temperature profile. It should be mentioned that increasing the negative wall slope of the temperature profile as a result of the increasing the heat generation effect causes the Nusselt number to increase as will be seen in the next paragraph. The opposite effect is obtained as the heat absorption effect is increased.

Fig. 4 shows the variations of the skin-friction coefficient C_f and the Nusselt number Nu against the dimensionless heat generation or absorption parameter Q for different values of the Prandtl number Pr and for certain values of $Sc = 0.6$, $\gamma = 1$, $R = 1$, $M = 1$ and $m = 0$. This is the case of destructive chemical reaction ($\gamma > 0$) with heat generation ($Q < 0$) or heat absorption ($Q > 0$). It is clear from this figure that increasing the heat generation or absorption parameter Q results in increases in the Nusselt numbers (as mentioned above) and decreases in the coefficient of friction. In addition, it is seen that the effect of increasing the Prandtl number is to enhance the heat transfer rate and to decrease the coefficient of friction due to reduction in the fluid velocity. It should be noted that as the Prandtl number increases, both the fluid temperature and velocity decrease. As a result, the negative wall slope of the temperature profile increases while the wall slope of the velocity profile decreases producing an increase in the Nusselt number and a decrease in the coefficient of friction as seen from Fig. 4. Also, for the parametric conditions used to produce Fig. 4, increasing Q increases the fluid temperature causing a more induced flow due to
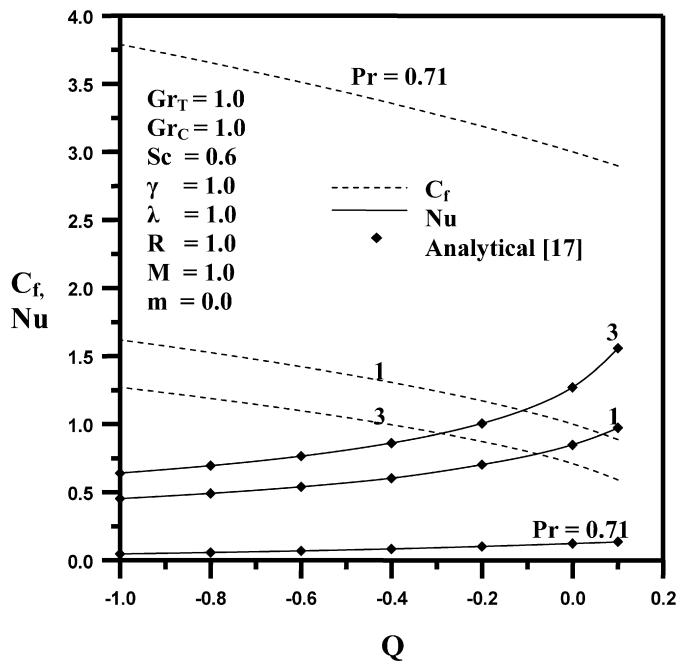
Fig. 4. Skin-friction coefficient and Nusselt number against dimensionless heat generation or absorption parameter for different Prandtl numbers.
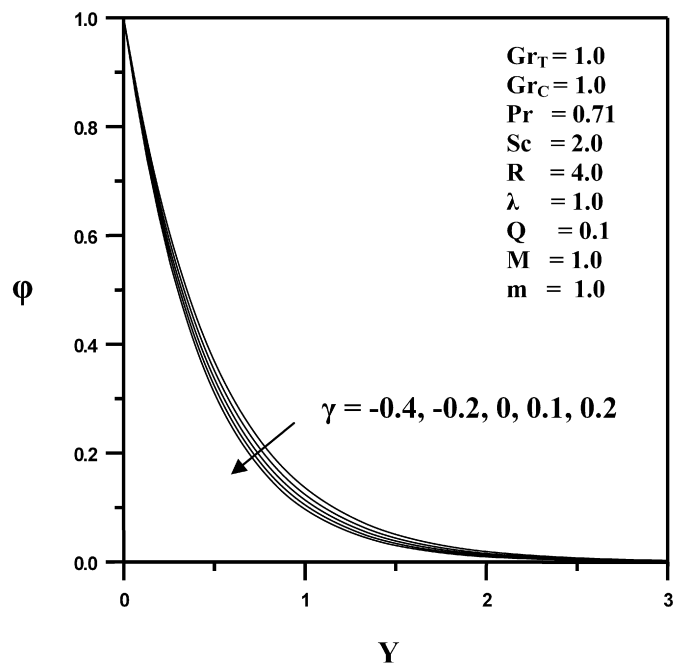

Fig. 6. Skin-friction coefficient and Sherwood number against dimensionless chemical reaction parameter for different Schmidt numbers.

dicted. It is interesting to note that in the presence of heat generation effect and a destructive chemical reaction, the negative wall slope of the concentration profile decreases yielding a decrease in the Sherwood number. However, in the presence of heat absorption and a destructive chemical reaction the negative wall slope of the concentration profile increases causing the Sherwood number to increase as seen in Fig. 6.

Fig. 6 elucidates the variations of skin-friction coefficient C_f and the Sherwood number Sh against the dimensionless chemical reaction parameter γ for different values of the Schmidt number and for certain values of $Pr = 0.71$, $Q = -0.4$, $R = 1$, $M = 1$, and $m = 0$. The range of the dimensionless chemical reaction parameter is considered from 0 to 2.0 (corresponding to the absence or presence of destructive chemical reaction) with heat absorption. This figure shows that increasing the value of the chemical reaction parameter increases the value of the Sherwood number and decreases that of the coefficient of friction due to reduction the wall slope of the velocity profile. Also, it is predicted that the mass transfer rate enhances while the coefficient of friction decreases as the Sherwood number increases.

4. Conclusions

The natural convection heat and mass transfer problem of a micropolar fluid past a vertical infinite permeable plate in the presence of a first-order chemical reaction and heat generation or absorption is studied. The governing equations are simplified by using a set of dimensionless variables and then solved numerically using the fourth-order Runge–Kutta method. It was found that, increasing the vortex viscosity parameter increased the coefficient of friction due to higher mixing of fluid layers, while the effect of increasing the micro-gyration vector caused a decrease in the coefficient of friction. Also, increasing the heat generation or absorption parameter and the chemical reaction parameter enhanced the respective heat and mass transfer coefficients or the Nusselt and Sherwood numbers and decreased the coefficient of friction. This same effect is also predicted by increasing the Prandtl and Schmidt numbers.

Fig. 5. Effect of chemical reaction parameter (γ) on concentration distribution.

the thermal buoyancy effect. However, the wall slope of the fluid velocity profile decreases producing a net decrease in the coefficient of friction as Q increases.

Fig. 5 displays typical concentration profiles for various values of the dimensionless chemical reaction parameter γ ranging from non-destructive ($\gamma < 0$) to destructive ($\gamma > 0$) chemical reactions in the presence of heat generation effect. The presence of a destructive chemical reaction within the boundary layer has the tendency to decrease the solute concentration. This accompanied by slight decreases in the solutal boundary layer thickness and the negative wall slope of the concentration profile. For non-destructive chemical reactions, the exact opposite effect is predicted.
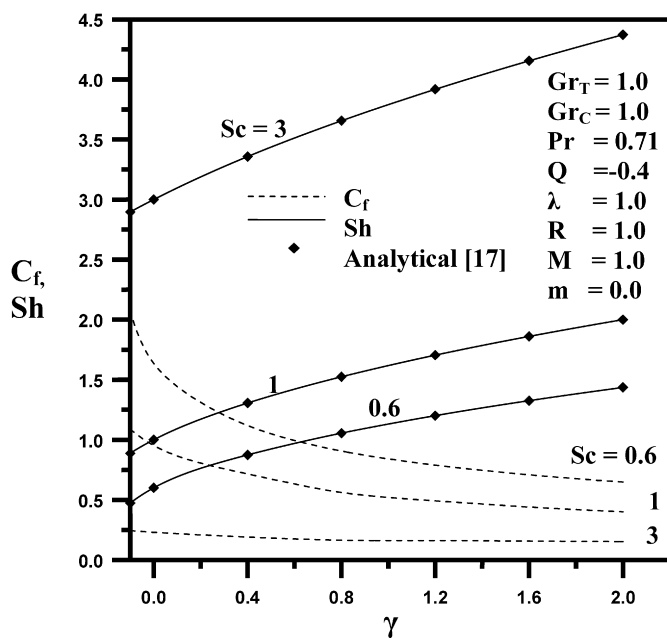
References

[1] A.C. Eringen, Theory of micropolar fluids, J. Math. Mech. 16 (1966) 1–18.

[2] A.C. Eringen, Theory of thermomicropolar fluids, J. Math. Anal. Appl. 38 (1972) 480–496.

[3] T. Ariman, M.A. Turk, N.D. Sylvester, Microcontinuum fluid mechanics. A review, Int. J. Eng. Sci. 11 (1973) 905–930.

[4] T. Ariman, M.A. Turk, N.D. Sylvester, Applications of microcontinuum fluid mechanics. A review, Int. J. Eng. Sci. 12 (1974) 273–293.

[5] G. Ahmadi, Self-similar solution of incompressible micro-polar boundary layer flow over a semi-infinite plate, Int. J. Eng. Sci. 14 (1976) 639–646.

[6] R.S.R. Gorla, R. Pender, J. Eppich, Heat transfer in micro-polar boundary layer flow over a flat plate, Int. J. Eng. Sci. 21 (1983) 791–798.

[7] R.S. Agarwal, C. Dhanapal, Flow and heat transfer in a micropolar fluid past a flat plate with suction and heat sources, Int. J. Eng. Sci. 26 (1988) 1257–1266.

[8] F.S. Lien, C.K. Chen, J.W. Cleaver, Analysis of natural convection flow of micropolar fluid about a sphere with blowing and suction, ASME J. Heat Transfer 108 (1986) 967–970.

[9] F.S. Lien, T.M. Chen, C.K. Chen, Analysis of free-convection micropolar boundary layer about a horizontal permeable cylinder at a non-uniform thermal condition, ASME J. Heat Transfer 112 (1990) 504–506.

[10] R. Nazar, N. Amin, I. Pop, Mixed convection boundary layer flow from a horizontal circular cylinder in a micropolar fluid: case of constant wall temperature, Int. J. Fluid Mechanics Research 31 (2004) 143–159.

[11] C.Y. Cheng, C.C. Wang, Forced convection in micropolar fluid flow over a wavy surface, Numerical Heat Transfer, Part A 37 (2000) 271–287.

[12] R. Bhargava, H.S. Takhar, Numerical study of heat transfer characteristics of the micropolar boundary layer near a stagnation point on a moving wall, Int. J. Eng. Sci. 38 (2000) 383–394.

[13] M.A. Mansour, M.A. Alhakiem, S.M. El Kabeir, Heat and mass transfer in magnetohydrodynamic flow of micropolar fluid on a circular cylinder with uniform heat and mass flux, J. Magnetism and Magnetic Materials 220 (2000) 259–270.

[14] N.A. Kelson, A. Desseaux, Effect on surface conditions on flow of a micropolar fluid driving by a porous stretching sheet, Int. J. Eng. Sci. 39 (2001) 1881–1897.

[15] F.S. Ibrahim, I.A. Hassanien, Local nonsimilarity solutions for mixed convection boundary layer flow of a micropolar fluid on horizontal flat plates with variable surface temperatures, Appl. Math. Comput. 122 (2001) 133–153.

[16] Y.J. Kim, J.C. Lee, Analytical studies on MHD oscillatory flow of a micropolar fluid over a vertical porous plate, Surface and Coating Technology 171 (2003) 187–193.

[17] A.J. Chamkha, MHD flow of a uniformly stretched vertical permeable surface in the presence of heat generation/absorption and a chemical reaction, Int. Comm. Heat Mass Transfer 30 (3) (2003) 413–422.

[18] R. Kandasamy, K. Periasamy, K.K.S. Prabhu, Chemical reaction, heat and mass transfer on MHD flow over a vertical stretching surface with heat source and thermal stratification effects, Int. J. Heat Mass Transfer 48 (2005) 4557–4561.

[19] R. Kandasamy, K. Periasamy, K.K.S. Prabhu, Effects of chemical reaction, heat and mass transfer along a wedge with heat source and concentration in the presence of suction or injection, Int. J. Heat Mass Transfer 48 (2005) 1388–1394.

[20] P.G. Siddheshwar, S. Manjunath, Unsteady convective diffusion with heterogeneous chemical reaction in a plane-Poiseuille flow of a micropolar fluid, Int. J. Eng. Science 38 (2000) 765–783.

[21] B.M. Mitrovic, D.V. Papavassiliou, Effects of a first-order chemical reaction on turbulent mass transfer, Int. J. Heat Mass Transfer 47 (2004) 34–61.

[22] Z. Chen, P. Arce, An integral-spectral approach for convective-diffusive mass transfer with chemical reaction in Couette flow. Mathematical formulation and numerical illustrations, Chem. Engrg. J. 68 (1997) 11–27.